Next-generation high-resolution borehole tensor strainmeters for the measurement of six strain-components based on fully automated interferometric displacement sensors

Jiayong Tian
National Institute of Natural Hazards, Ministry of Emergency Management of P.R.China, Beijing, P.R.China

Kanghua Zhang
Tianjin University, Tianjin, P.R.China

Jiashu Lou
National Institute of Natural Hazards, Ministry of Emergency Management of P.R.China, Beijing, P.R.China

ABSTRACT: Conventional borehole tensor strainmeters (BTSM) based on the measurement of inner-diameter changes of strainmeters by four capacitance gauges had been developed to measure three strain-components in the horizontal plane. The other three strain components are also important, but are difficult to implement because of large volume of sensors. In order to measure six strain-components completely, we develop a new high-resolution BTSM based on a fully automated interferometric displacement sensor with fibre-based heads of the millimeter dimension,which makes the gauge ultra-compact to implement the four inner-diameter-change measurement and other three-gauge measurements considering the influences of strain components in the plane of vertical normal. Compared with conventional BTSM, the impulse hammer test results show that gauge design of the new BTSM extends measurement resolution from 10^{-9} to 10^{-12} and increases the measurement bandwidth greatly, which advances the technology of borehole strain.

Keywords: *High-resolution borehole tensor strainmeters, Fully automated interferometric displacement sensors, six strain-components, Next-generation.*

1 INTRODUCTION

Based on the inner-diameter-change measurement of the stainless-steel casing by four three-element-capacitance gauges, the conventional high-resolution borehole tensor strainmeters (BTSM), for example, RZB-type (OuYang *et al.*, 2009), YRY-type (Chi, 1993), and GTSM-type strainmeters (Gladwin and Hart, 1985), had been developed to measure three crustal-strain components in the horizontal plane. These BTSMs had been deployed into Plate Boundary Observatory (PBO) (Roeloffs, 2010, Hodgkinson *et al.*, 2013) and China Borehole-strain Observatory (CBSO) to investigate ground deformation induced by fault slip, earthquake, volcanic activity, and Earth tide, etc. Usually, each three-element-capacitance gauge is an independent module of the length of 170 mm, where the length of BTSM is more than 680 mm. When the BTSM is installed in the shallow borehole to measure the low-frequency signals, the theoretical measurement model of the conventional BTSM can be described as the quasi-static plane stress model of stress concentration around the borehole. But with the increase of the installation depth of BTSM and signal frequency,

the theoretical measurement model of the conventional BTSM will fail because the other three strain components including the normal- and shear-strain components in the plane of vertical normal will contribute the response of the conventional BTSM greatly (Zhang *et al.*, 2019, Zhang *et al.*, 2020, Zhang *et al.*, 2021). The non-conplanar measurement of four three-element-capacitance gauges may also cause significant errors. Furthermore, in case of lighting struck and cable failure, the electronical-based design in the downhole system will induce complete failure of the BTSM, which means that it is difficult to guarantee adequate performance beyond about 20-25 years and total cost for the borehole strain observation is too expensive to conduct operational observation. Therefore, quantitative observation of high-resolution and high-frequency crustal strain tensor for the relevant investigation in geodynamics, seismology, and dynamics of natural hazards demands the new-generation high-resolution BTSM (Gladwin and Hart, 1985).

In order to advance the technology of borehole strain observation, a new high-resolution BTSM based on attocube atto FPS3010 system has been deveopled in this paper. Firstly, theoretical model of six strain-component measurement for the BTSM is given briefly. Secondly, based on attocube atto FPS3010 interferometric displacement sensor in conjunction with fibre-based sensor heads (attocube-systems-AG, 2023b, attocube-systems-AG, 2023a), the guage arrangement of the new BTSM is presnted to implement the high-resolution and high-frequency con-planar measurement of seven gauges inside the stainless-steel casing of 78 mm inner diameter to reflect six components of crustal-strain tensor. Lastly, the impulse hamber test is used to verify effectiveness of the gauge design in the new BTSM.

2 THEORETICAL MODEL OF SIX STRAIN-COMPONENT MEASUREMENT FOR THE BTSM

In the conventional BTSM, four-gauge arrangements are used to measure relative change of borehole diameter $U_r(\theta_j,z)$ to only reflect the influence of three strain components in the plane of horizontal normal. Besides these four-gauge arrangements, the other three gauges $U_{zr}(\theta_5,z)$, $U_{zr}(\theta_6,z)$, and $U_z(\theta_7,z)$ are introduced to reflect the influence of three strain components in the plane of vertical normal (Tian *et al.*, 2023),

$$\left.\begin{aligned} U_r(\theta_j,z) &= \frac{u_r(a,\theta_j,z)+u_r(a,\theta_j+\pi,z)}{2a}, \quad j=1,2,3,4 \\ U_{zr}(\theta_j,z) &= \frac{1}{2}\left(\frac{u_z(a,\theta_j,z)-u_z(a,\theta_j+\pi,z)}{2a}+\frac{u_r(a,\theta_j,z)-u_r(a,\theta_j,z_{rj})}{z-z_{rj}}\right), \quad j=5,6 \\ U_z(\theta_j,z) &= \frac{u_z\left(a,\theta_j,z+\frac{h_0}{2}\right)-u_z\left(a,\theta_j,z-\frac{h_0}{2}\right)}{h_0}, j=7 \end{aligned}\right\}, \tag{1}$$

where $U_r(\theta_j,z)$, $U_{zr}(\theta_j,z)$,and $U_z(\theta_j,z)$ are relative change of borehole diameter at azimuth angle θ_j, sum of relative change of vertical displacements between θ_j and $\theta_j+\pi$ at z and relative change of borehole diameter between z and z_{rj} at θ_j, and relative change of the vertical displacements between $z+\frac{h_0}{2}$ and $z-\frac{h_0}{2}$ at azimuth angle θ_j,respectively .

To eliminate the influence of gauge arrangements as soon as possible, instrumental strains $\boldsymbol{\varepsilon}^I$ are introduced to be related to gauge responses $\mathbf{e}$ by gauge orientation matrix $\mathbf{O}$ as

$$\mathbf{e}=\mathbf{O}\boldsymbol{\varepsilon}^I, \tag{2}$$

where

$$\mathbf{e}=\left[U_r(\theta_1,z)\quad U_r(\theta_2,z)\quad U_r(\theta_3,z)\quad U_r(\theta_4,z)\quad U_{zr}(\theta_5,z)\quad U_{zr}(\theta_6,z)\quad U_z(\theta_7,z)\right]^T,$$

$$\boldsymbol{\varepsilon}^I=\left[\varepsilon_{xx}^I+\varepsilon_{yy}^I\quad \varepsilon_{xx}^I-\varepsilon_{yy}^I\quad \varepsilon_{xy}^I\quad \varepsilon_{xz}^I\quad \varepsilon_{yz}^I\quad \varepsilon_{zz}^I\right]^T,$$

$$\mathbf{O}=\begin{bmatrix}1/2 & 1/2\cos(2\theta_1) & \sin(2\theta_1) & 0 & 0 & 0\\ 1/2 & 1/2\cos(2\theta_2) & \sin(2\theta_2) & 0 & 0 & 0\\ 1/2 & 1/2\cos(2\theta_3) & \sin(2\theta_3) & 0 & 0 & 0\\ 1/2 & 1/2\cos(2\theta_4) & \sin(2\theta_4) & 0 & 0 & 0\\ 0 & 0 & 0 & \cos(\theta_5) & \sin(\theta_5) & 0\\ 0 & 0 & 0 & \cos(\theta_6) & \sin(\theta_6) & 0\\ 0 & 0 & 0 & 0 & 0 & 1\end{bmatrix}.$$

Instrumental strain $\boldsymbol{\varepsilon}^I$ could be further related to strain components induced by the incident strain wave $\boldsymbol{\varepsilon}^i$ by calibration matrix $\mathbf{K}$ as

$$\boldsymbol{\varepsilon}^I=\mathbf{K}\boldsymbol{\varepsilon}^i, \tag{3}$$

where $\boldsymbol{\varepsilon}^i=\left[\varepsilon_{xx}^i+\varepsilon_{yy}^i\quad \varepsilon_{xx}^i-\varepsilon_{yy}^i\quad \varepsilon_{xy}^i\quad \varepsilon_{xz}^i\quad \varepsilon_{yz}^i\quad \varepsilon_{zz}^i\right]^T$. Calibration matrix $\mathbf{K}$ is determined by Poisson ratio v of surrounding rock, non-dimensional wave number k_pa or k_sa of the incident waves, the azimuth angle θ_i of gauges, and the incident angles of the incident wave.

3 GAUGE DESIGN OF THE NEW BTSM BASED ON INTERFEROMETRIC DISPLACEMENT SENSOR

In order to implement the high-resolution and high-frequency con-planar measurement of seven gauges shown in Eq.(1) inside the stainless-steel casing of 78mm inner diameter to reflect six components of crustal-strain tensor in the new BTSM, attocube atto FPS3010 system, as a fully automated interferometric displacement sensor in conjunction with millimeter-sized fiber-based sensor head, is introduced by the special design of optical path in the gauges. The measurement resolution and bandwidth of FPS sensor are 1pm and 10MHz, respectively.

Figure 1 shows gauge arrangements for the new BTSM and its inside view. Following the gauge arrangement of GTSM-type BTSM, gauges 1-4 measure the inner-diameter changes of stainless-steel casing at azimuth angles 0°, 60°, 120°, and 150°, respectively. Gauges 5 and 6 measure the sum of u_r-change at casing wall with relative to z and u_z-change at casing wall with relative to casing inner-diameter at azimuth angles 90° and 135°, respectively. Gauge 7 is for the measurement of u_z-change at casing wall along the casing axis at azimuth angle 210°.

The design of gauges 1-4 and 7 is shown in Fig.2. In gauges 1-4, sensor head is mounted downward on a rigid frame to measure the change of inner diameter by the beam reflection by a 45^0 polished stainless-steel surface below the sensor and a 90^0 polished surface mounted on the opposite wall. Such optical-path design of gauges 1-4 means that it is difficult to make the conventional alignment of beam path inside the casing after the installation of the gauges. But standard FPS heads admits alignment angle tolerances as large as 3.5 mrad, which promises no alignment of beam path under the control of the common installation and machining precision. In gauge 7, the sensor head is installed downward to measure the vertical displacement by the beam reflection by one polished stainless-steel surface installed below the sensor.

Figure 3 shows the design of gauges 5 and 6. Gauges 5 and 6 include two sub-gauges, respectively. In gauge 5, sub-gauge A and sub-gauge B measures u_z-change at borehole wall with relative to the inner diameter of the casing wall and u_r-change at casing wall with relative to z, respectively. In gauge 6, sub-gauge C and sub-gauge D measure u_r-change at casing wall with relative to z and u_z-change at borehole wall with relative to the inner diameter of the casing wall, respectively.

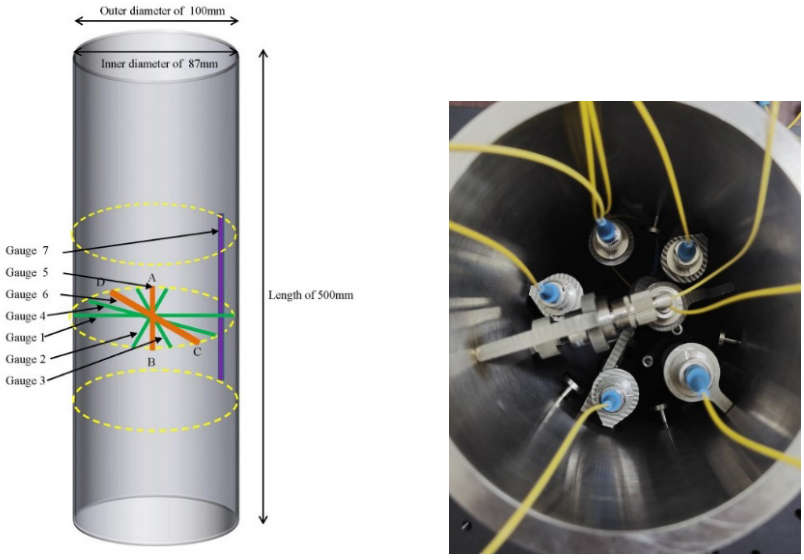

(a) gauge arrangements (b) inside view

Figure 1. Schematic diagram for gauge arrangements for the new BTSM.

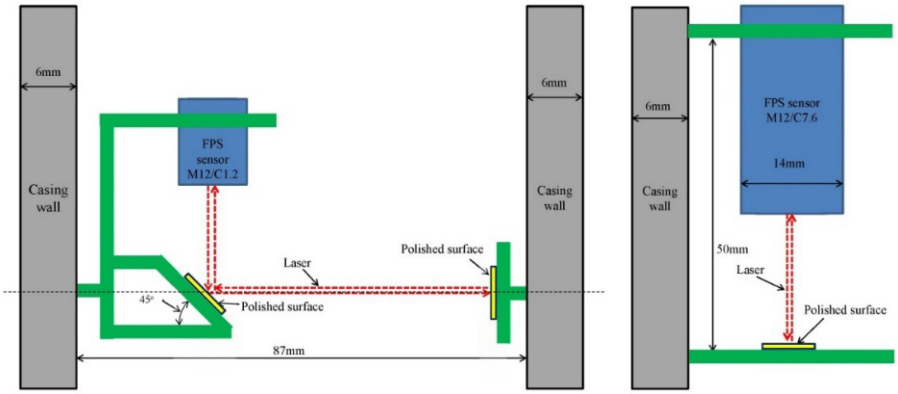

(a) Gauges 1-4 (b) Gauge 7

Figure 2. Schematic diagram for the optical design of gauges 1-4 and 7.

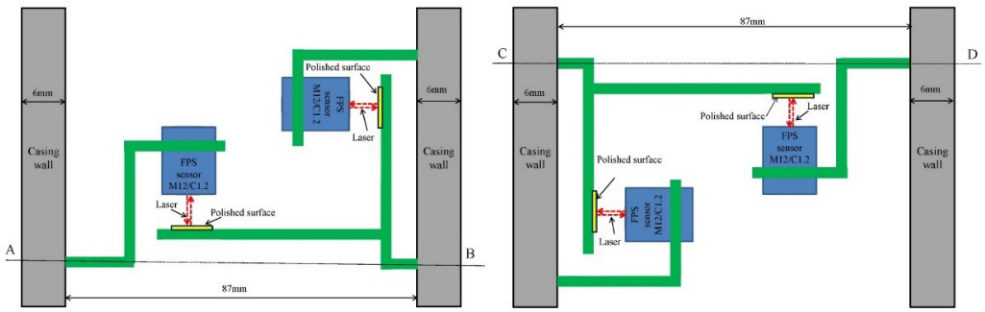

(a) Gauge 5 (Sub-gauges A and B) (b) Gauge 6 (Sub-gauges C and D)

Figure 3. Schematic diagram for the optical design of gauges 5 and 6.

4 RESULTS AND DISCUSSSIONS

In order to verify effectiveness of the gauge design in the new BTSM, impulse hammer test is adopted to record the gauge responses. Figure 5 shows the gauge measurement results in the impulse hammer test. Because the present attocube atto FPS3010 system can only provide 3 sensor axes, therefore only the responses of three gauges could be recorded simultaneously for one impulse hammer test.

Gauges 1-3, gauges 4 and 7, gauges A and B, and gauges C and D are set as one group for the test, respectively. The measurement results of gauges 1-3 are shown in Fig.5(a). Here gauge-4 result is also included in Fig.5(a) in order to compare with gauges 1-3. It is shown in Fig.5(a) that the responses of gauges 1-4 can be recorded clearly by the present design, where the recorded maximum displacements are tens nanometers. Fig.5(b) gives the responses of gauges 4 and 7, where the response of gauge 7 is much larger than that of gauge 4 because radial stiffness of steel casing is much more than axial stiffness of the steel casing. Fig.5(c) and (d) give the responses of gauges A-B and C-D, respectively. Response of gauge B is about 40 times of that of gauge A. Responses of gauges C and D are the same order. Although the present measurement bandwidth of these gauges cannot measure quantitatively, the theoretical 0.1dB bandwidth of these gauges is estimated as more than 200Hz according to the calculation of free vibration of Timoshenko-beam model.

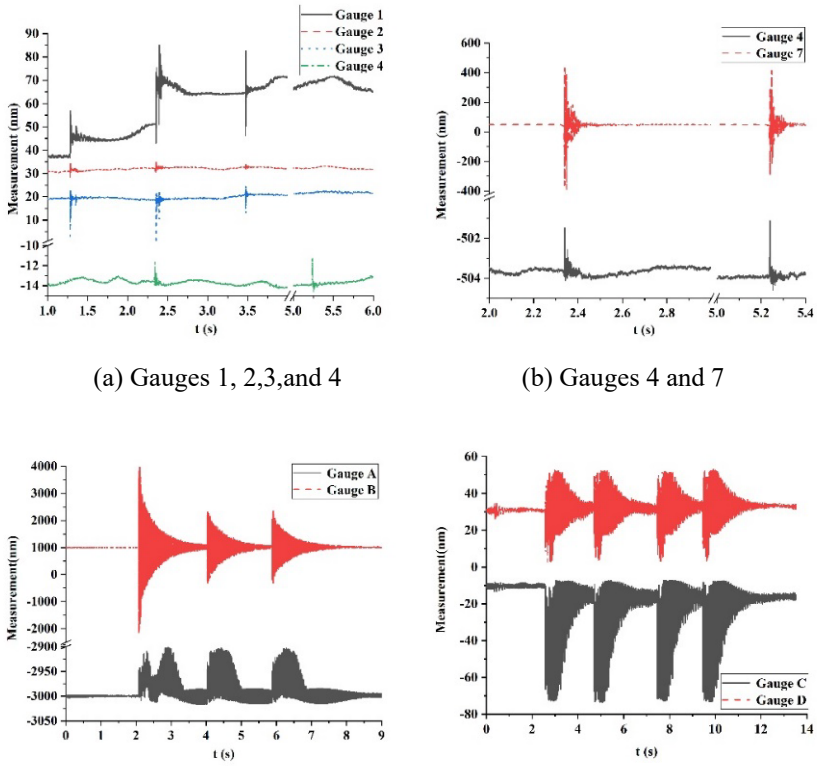

(a) Gauges 1, 2,3,and 4 (b) Gauges 4 and 7

(c) Sub-gauges A and B (d) Sub-gauges C and D

Figure 4. Measurement results of the gauges in the impulse hammer test.

5 CONCLUSIONS

In this paper, the new high-resolution BTSM based on the interferometric displacement sensor in conjunction with fibre-based sensor heads has been developed. Millimeter-sized of sensor heads implement the high-resolution and high-frequency con-planar measurement of seven gauges inside the stainless-steel casing of 78 mm inner diameter to reflect six components of crustal-strain tensor in the new BTSM, which could make the length of the BTSM decreases greatly. Compared with the conventional BTSM, the test results show that the present gauge design of the new BTSM extend measurement resolution from 10^{-9} to 10^{-12} and the bandwidth from 20Hz to more than 200Hz , and have excellent repeatability of the strain measurement, which means that the new BTSM not only advance the technology of borehole strain observation but also benefit the relevant investigation of geodynamics, high-frequency seismology, and engineering application.

ACKNOWLEDGEMENTS

The authors kindly acknowledge the support of research grants from National Institute of Natural Hazards, Ministry of Emergency Management of P.R.China (ZDJ2019-15-1 and ZDJ2018-22).

REFERENCES

Attocube-Systems-Ag, 2023a. *FPS 3010* [online]. https://www.attocube.com/en/ressources/brochures

Attocube-Systems-Ag, 2023b. *FPS sensor* [online]. https://www.attocube.com/en/products/laser-displacement-sensor

Chi, S.L., 1993. Trial results of YRY-2 shallow borehole strainmeter at eight observation sites in North China. *Earthquake Science,* 6**,** 731-737.

Gladwin, M.T. & Hart, R., 1985. Design parameters for borehole strain instrumentation. *Pure & Applied Geophysics,* 123**,** 59-80.

Hodgkinson, K., Langbein, J., Henderson, B., Mencin, D. & Borsa, A., 2013. Tidal calibration of plate boundary observatory borehole strainmeters. *Journal of Geophysical Research: Solid Earth,* 118**,** 447-458.

Ouyang, Z.X., Zhang, H.X., Fu, Z.Z., Gou, B. & Jiang, W.L., 2009. Abnormal phenomena recorded by several earthquake precursor observation instruments before the M(s) 8.0 Wenchuan, Sichuan earthquake. *Acta Geologica Sinica - English Edition,* 83**,** 834-844.

Roeloffs, E., 2010. Tidal calibration of Plate Boundary Observatory borehole strainmeters: Roles of vertical and shear coupling. *Journal of Geophysical Research: Solid Earth,* 115**,** B06405.

Tian, J., Zhang, K. & Lou, J., 2023. Instrumental response of borehole tensor strainmeters for oblique-incident seismic waves. *IOP Conference Series: Earth and Environmental Science,* 1124**,** 012074.

Zhang, K., Tian, J. & Hu, Z., 2019. Theoretical frequency response bandwidth of empty borehole for the measurement of strain waves in borehole tensor strainmeters. *Bulletin of the Seismological Society of America,* 109**,** 2459-2469.

Zhang, K., Tian, J. & Hu, Z., 2020. The influence of the expansive grout on theoretical bandwidth for the measurement of strain waves by borehole tensor strainmeters. *Applied Sciences,* 10**,** 3199.

Zhang, K., Tian, J. & Hu, Z., 2021. Can Seismic Strain Waves Be Measured Quantitatively by Borehole Tensor Strainmeters? *Seismological Research Letters,* 92**,** 3602-3609.